Four-pion state in UPC

Mariola Kłusek-Gawenda
Institute of Nuclear Physics Polish Academy of Sciences,
Radzikowskiego 152, PL-31-342 Kraków, Poland

The production of $2\pi^+2\pi^-$ in ultraperipheral heavy-ion collisions at RHIC and LHC energies is studied. Preliminary H1 data is used to enhance the understanding of the poorly known process. Predictions for photon-nucleus interactions are calculated for various excited states of mesons. Agreement between theoretical predictions and available STAR data at RHIC is presented. The comparison of the $2\pi^+2\pi^-$ invariant mass spectrum and nuclear total cross section indicates that $\rho(1570)$ plays a crucial role in accurately describing existing experimental data. Nuclear predictions for LHC energy in the central region of rapidity are also provided.

DOI: https://doi.org/10.17161/bc489f93
Keywords: Heavy ion ultraperipheral collisions, rho meson, four-pion production

1 Motivation

The exclusive production of four charged pions is an area of growing interest within the field of particle physics. This process, particularly in the context of ultraperipheral heavy-ion collisions and photoproduction, provides a unique opportunity to explore a variety of fundamental aspects of the underlying physics. These include resonance production, and searches for exotic resonances. In recent studies, the H1 collaboration at HERA [1] has presented preliminary data on exclusive four-pion production, marking a significant step forward in our understanding of this complex process. This data, along with earlier findings from the STAR Collaboration [2], highlights the potential of studying this decay mode to uncover the characteristics of various resonances that contribute to the process. Furthermore, the exclusive production of four charged pions at low photon virtualities ($Q^2 < 2$ GeV^2) and in ultraperipheral heavy-ion collisions offers an opportunity to observe coherent photoproduction and the behavior of vector mesons such as $\rho(1450)$, $\rho(1570)$, $\rho^0(1700)$. The invariant mass spectrum associated with this production often reveals broad peaks, providing crucial insights into the properties of mesonic states.

The motivation for this study stems from findings presented by the H1 collaboration, which suggest intriguing avenues for further investigation. By studying four charged pion photoproduction at LHC energies, we aim to make predictions and contribute valuable insights to this evolving field [3].

2 Meson photonuclear production

Vector meson photoproduction is a key area of study in particle physics, particularly for understanding the interactions between photons and protons. One commonly used theoretical framework for this process is the vector meson dominance model (VDM) [4,5]. The photon is treated as fluctuating into a hadronic state that can interact with a proton through Pomeron or Reggeon exchange. The VDM provides a way to describe the behavior of the photon in terms of vector mesons, which mediate the interaction with the proton. This approach has been successful in explaining various aspects of photoproduction and scattering processes. For instance, the proton, meson, or photon ($X = p, V, \gamma$ respectively) cross sections can be modeled using the Donnachie and Landshoff model [6], which accounts for exchanges through Pomeron and Reggeon trajectories. Through VDM, the total cross section dependence can be analyzed, allowing researchers to gain insights into the underlying dynamics of vector meson photoproduction. The

dependence of the total cross section on the two main trajectories can be expressed as follows

$$\sigma_{tot}(Xp) = \alpha_1 W_{\gamma p}^{-\delta_1} + \alpha_2 W_{\gamma p}^{\delta_2} \,. \tag{1}$$

The component with a negative power corresponds to the Reggeon exchange, specifically involving the exchange of mesons such as ρ, ω, f and a. The second term in Eq. 1 arises from the Pomeron exchange, which becomes dominant at sufficiently high energies. By analogy with the Reggeon and Pomeron exchange, the cross section for exclusive vector meson production can be determined. The CMS Collaboration measured exclusive $\rho^0(770)$ meson photoproduction in ultraperipheral $p-Pb$ collisions at a center-of-mass energy of 5.02 TeV [7]. Their measurements of δ_1 and δ_2 are utilized in this analysis.

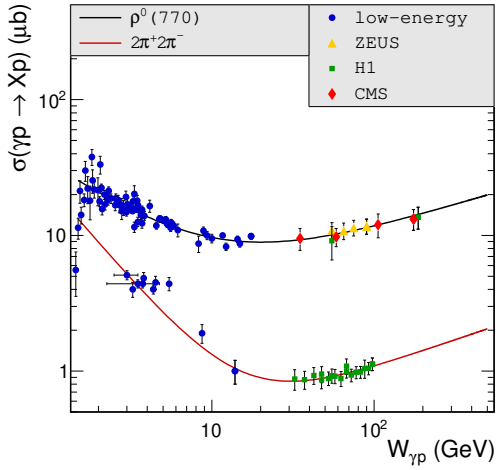

Figure 1 – Total cross section for the exclusive production of $\rho^0(770)$ vector meson (upper line) and $2\pi^+2\pi^-$ production (lower line). The parametrization of low-energy [8,9,10,11] and high-energy $\rho^0(770)$ data [12,13,7] as well as low-energy [14,15,16,17,18] and preliminary H1 four-charged-pion data [1] are presented.

Fig. 1 shows the total cross section for exclusive photoproduction of $\rho^0(770)$ vector meson and the $2\pi^+2\pi^-$ state. The low-energy data (blue circular points), with $W_{\gamma p} < 20$ GeV, were obtained using fixed-target experiments. The cross section for the $\sigma(\gamma p \to \rho^0(770)p)$ process was measured at an average energy of $< W_{\gamma p} >= 92.6$ GeV by the CMS Collaboration and found to be 11.2 ± 1.4 (stat) ± 1.0 (syst.) μb. The CMS measurement aligns with the previous data [8,9,10]. The data show good agreement with our calculations, particularly at HERA and LHC energies

Due to the limited experimental data on four-pion production, there is no consensus on which resonance states play the most significant role. At low $W_{\gamma p}$ energies (less than 3 GeV), the non-resonant signal dominates, while excited states of the ρ meson become important for $W_{\gamma p} > 4$ GeV. Such resonances should be considered in the context of $\pi^+\pi^-\pi^+\pi^-$ production at HERA, RHIC, and LHC energies. A simple fit to H1 data [1] demonstrated that a combination of the Breit-Wigner $\rho(1570)$ resonant, non-resonant four-pion state, and complex phase ($\rho(1570) - 4\pi$ interference) adequately describes the experimental points. From the four-pion invariant mass distribution ($M_{4\pi}$), it can be inferred that a single broad $\rho(1570)$ resonance is the most significant in the photoproduction of exclusive $2\pi^+2\pi^-$ final states. Additionally, data reveals a correlation in the four-pion invariant mass of oppositely charged pions, suggesting an enhancement of the four-pion signal around $M_{4\pi} = 1450$ and 1700 MeV. These correspond to the $\rho(1450) \equiv \rho'$ and $\rho(1700) \equiv \rho''$ states. Unfortunately, the branching rates of these resonances to four-pion states remain uncertain, limiting our ability to accurately determine these factors. Similarly, the branching ratio for $\rho \to e^+e^-$ is another value lacking precision. Table 1 shows the mass and width of resonances [19] as well as estimated values of $\Gamma(V \to e^+e^-)$ used in this analysis.

In the VDM-Regge approach, the photon state $|\gamma>$ is considered aquantum mechanical superposition of the quantum electrodynamics photon state $|\gamma_{QED}>$ and a hadronic state $|h>$:

$$|\gamma >= \mathcal{N}|\gamma_{QED} > + |h> \text{ , where } |h >= \sum_h \frac{e}{f_V}|V> \ . \tag{2}$$

The vector meson-photon coupling , represented by $f_V^2 = \frac{e^2 \alpha_{em} m_V}{3\Gamma(V \to e^+e^-)}$, is derived from the e^+e^- decay width of the vector meson with m_V mass. The constant factor f_V is independent of Q^2 and represents

Table 1: Characteristic of the ρ', $\rho(1570)$ and ρ'' mesons.

Resonance	m [GeV]	Γ [GeV]	$\Gamma_{e^+e^-}$ [keV]
$\rho(1450)$	1.465 ± 0.025	0.4 ± 0.05	$4.30 - 10$
$\rho(1570)$	1.570 ± 0.070	0.144 ± 0.09	$0.35 - 0.5$
$\rho(1700)$	1.720 ± 0.020	0.25 ± 0.01	$6.30 - 8.9$

the probability of the photon transitioning into a vector meson. The normalization factor $\mathcal{N}$ in Eq. (2) ensured the proper balance of the superposition. The hadronic state $|h>$ is expected to have the same additive quantum numbers as the photon, with $J^{PC} = 1^{--}$, and $Q = B = S = 0$ for vector meson. The QED component on its own does not interact with hadrons [20]. Notably, the primary contributions to the hadronic component $|V>$ come from the light vector mesons (ρ^0, ω and ϕ), which forms the central hypothesis of the VDM approach. The straightforward VDM-Regge approach enables the description of the photon-to-vector meson transition using the relation of the photon-proton cross section. Given that H1 data does not provide differential cross sections in the square of the momentum transfer for the $\gamma p \to 2\pi^+2\pi^- p$ process, we have used $\sigma(\gamma p \to 2\pi^+2\pi^- p)$ as the baseline for this analysis. In the VMD-Regge model, the total cross section for Vp photoproduction can be calculated through the optical theorem considering the forward $\gamma p \to Vp$ cross section:

$$\sigma_{tot}(Vp) = \frac{f_V^2}{e^2}\sigma(\gamma p \to Vp) \, . \tag{3}$$

Our simple calculation effectively models the experimental data for $\sigma(\gamma p \to 2\pi^+2\pi^- p)$ (see Fig. 1), particularly at the energy levels relevant to H1.

Photoproduction of vector mesons on the nucleus can be considered by integrating the VDM-Regge model with the Glauber theory of multiple scattering [21]. The total cross section for light vector meson–nucleus interaction is computed using the nuclear optical density normalized to unity ($T_A(\vec{b}) = \int_{-\infty}^{+\infty} \rho(\vec{b}, z)\mathrm{d}z$) in the following equation [22]:

$$\sigma_{tot}(VA) = \int \left[1 - \exp\left(-\sigma_{tot}\,(Vp)\, T_A(\vec{b})\right)\right] \mathrm{d}^2 b \tag{4}$$

The two-parameter Fermi model is employed to represent the densities of gold and lead nuclei [23]. The charge distribution within the nucleus is adjusted to match the mass number using the relation: $\int \mathrm{d}^2 b \rho(b, z)\mathrm{d}z = A$. Eq. (4) is framed within the "classical mechanics" context. It's important to mention that the "quantum expression" is also frequently referenced in literature. Nonetheless, as detailed in Ref. [26], for coherent J/ψ photoproduction in ultraperipheral collisions, there is approximately a 15% deviation between these two different rescattering approaches. Additionally, the discrepancy between the methods increases when considering $\rho^0(770)$ photoproduction [27]. The formula for coherent vector meson photoproduction on nuclei is as follows:

$$\sigma\left(\gamma A \to VA\right) = \frac{1}{16\pi}\frac{e^2}{f_V^2}\sigma_{tot}^2\left(VA\right)\int |F(t)|^2 \, \mathrm{d}t \, . \tag{5}$$

The nuclear form factor is expressed through charge distribution in the nucleus. Here we use the so-called realistic form factor. See *e.g.* Ref. [24] for more details.

Fig. 2(a) illustrates the cross section for the photoproduction of two- and four-pion state, particularly for the lead nucleus. The highest cross section is observed when the $\rho^0(770)$ meson decays into the $\pi^+\pi^-$ channel. The theoretical model, which includes the classical approach of ρ^0 photoproduction (Eq. (4)), aligns well with the LHC experimental data. We present two datasets from the STAR collaboration at RHIC. The first dataset (represented by green triangular points) has been utilized in numerous theoretical and phenomenological studies on $\rho^0(770)$ photoproduction, such as Ref. [32]. Our parametrization agrees with these calculations, while Ref. [33] identifies a slight discrepancy with other approaches. The new data points provide an estimation of STAR data for $Au - Au$ collision energies of 62.4, 130, and 200 GeV. The mid-rapidity cross section is as follows:

$$\sigma(\gamma A \to VA; y = 0) = \frac{1}{N_{\gamma A}(y = 0)}\frac{\mathrm{d}\sigma(AA \to AAV; y = 0)}{\mathrm{d}y} \, . \tag{6}$$

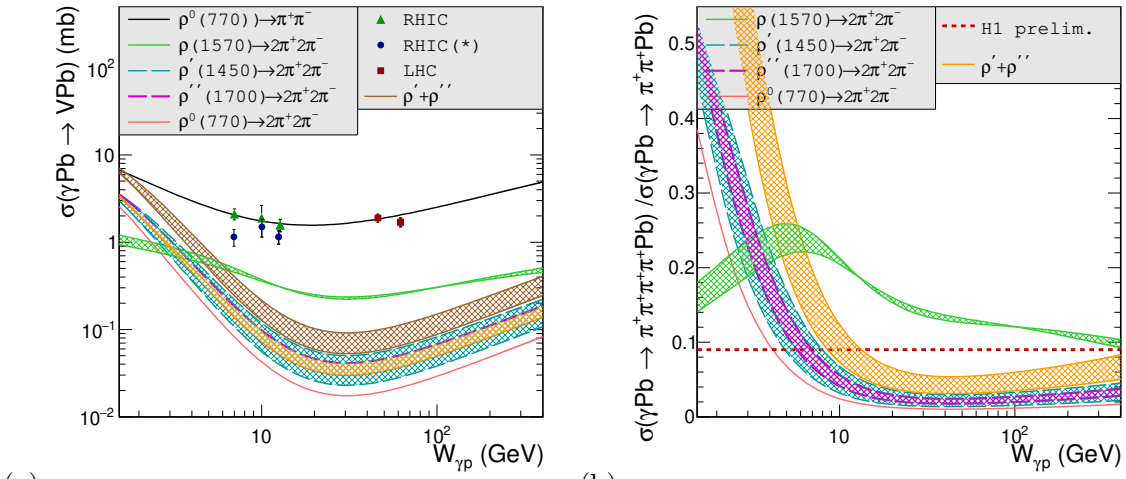

Figure 2 – (a) Cross section for the $\gamma Pb \to VPb$ process. The upper black line shows the results for $V = \rho^0(770)$ that decays into two charged pions. Lowers curves correspond to $2\pi^+2\pi^-$ production. Results for $\gamma Pb \to \pi^+\pi^- Pb$ are compared with existing experimental data [28,35,30,31]. (b) Ratio of four to two charged pions photoproduction. The theoretical results are compared with the recent H1 preliminary data [1].

Results set has been calculated using so-called realistic form factor. The flux of equivalent photons is heavily dependent on the charge distribution within the nucleus, especially at small impact parameters. This subject requires further detailed investigation in subsequent studies.

The branching ratios of excited ρ states are not well established. The final result of the photonuclear section depends on this limit. Fig. 2 shows band of uncertainty correspond to the decay of $\rho', \rho'', \rho(1570)$ into 4 charged pions. At low photon-nucleus energies, the combined contribution of ρ' and ρ'' surpasses the impact of the $\rho(1570) \to 4\pi$ decay. The $\gamma Pb \to \rho(1570)Pb$ cross section starts to dominate over other excited states only when $W_{\gamma p}$ is above 8 GeV. The lowest curve is associated with the $\rho^0(770)$ meson, which decays into a four-charged-pion channel. The difference in distribution between two- and four-pion states from ρ^0 decay can vary by as much as two orders of magnitude. Fig. 2(b) illustrates the ratio of $\pi^+\pi^-\pi^+\pi^-$ to $\pi^+\pi^-$ photoproduction. Theoretical results are compared with preliminary H1 data, which is around 9% [1]. The range of $W_{\gamma p}$ energy used for photoproduction at LHC energy is approximately 10 GeV for $y = -4$ and 650 GeV for $y = 4$. For the decay of $\rho(1570) \to 2\pi^+2\pi^-$ at mid-rapidity, the energy is around 90 GeV. While our results do not perfectly match the H1 value, they are close to it. The results for $\rho(1570)$ tend to overestimate the data, whereas the combined sum of ρ' and ρ'' is less than the preliminary H1 point in the energy range that aligns with LHC measurements

3 Cross sections for nuclear four-pion production

Nuclear photoproduction of a vector meson V can be expressed as the combination of the photonuclear cross section Eq. (5) and equivalent photons fluxes:

$$\frac{\mathrm{d}\sigma(AA \to AAV)}{\mathrm{d}^2b\mathrm{d}y} = \omega_1 N(\omega_1, b)\sigma(\gamma A_2 \to VA_2) + \omega_2 N(\omega_2, b)\sigma(\gamma A_1 \to VA_1)\ , \tag{7}$$

In the equation, $\omega_i = m_V/2exp(\pm y)$ represents the energy of emitted photon, while b stands for the impact parameter. We focus on ultraperipheral collisions, implying that transverse distance between the centers of the nuclei is larger than the sum of the radii of nuclei [25]. The photon flux depends on the form factor, specially on the charge distribution within the nucleus. For a detailed analysis of the model for vector meson photoproduction, refer to [26,34]. Eq. (7) allows the calculation of both total and differentail cross section as a function of the rapidity of outgoing photon or impact parameter. A comprehensive analysis should also account for the kinematics of the decay products. In the study of four-pion production, the rapidity of each outgoing pion must be considered, achieved by accounting for the smearing of ρ mesons. The widths of ρ', ρ'', and $\rho(1570)$ are knows, see Table 1. The primary part of the vector meson's spectral shape is derived from the Breit-Wigner formula:

$$\mathcal{A} = \mathcal{A}_{BW}\frac{\sqrt{mm_V\Gamma(m)}}{m^2 - m_V^2 + im_V\Gamma(m)} + \mathcal{A}_{bkg}\ . \tag{8}$$

The mass-dependent width is expressed using the following formula:

$$\Gamma(m) = \Gamma_V \frac{m_V}{m} \left(\frac{m^2 - 4m_V^2}{m_V^2 - 4m_\pi^2} \right)^{\frac{3}{2}} . \tag{9}$$

A term $\mathcal{A}_{bkg}$ is understood to represent the background contribution from $\pi^+\pi^-$ production. This factor accounts for the enhancement on the left side of the resonance term and some blurring on the right side. Ideally, data including the rapidity of each decay particle would allow for a thorough kinematic study of the $1 \to 4$ process. For simplicity, we consider the $1 \to 4$ state as a two-step process: $1 \to 2 \to 4$:

$$\sigma(AA \to AAV \to AA\pi^+\pi^-\pi^+\pi^-, y_V) = \mathcal{C} \times \tag{10}$$
$$\left[\sigma(AA \to AAV \to AA\pi^+\pi^-\pi^+\pi^-; y_{\pi_1} y_{\pi_2}) \times \right. \tag{11}$$
$$\left. \sigma(AA \to AAV \to AA\pi^+\pi^-\pi^+\pi^-; y_{\pi_3} y_{\pi_4}) \right] .$$

The normalization constant $\mathcal{C}$ varies for each excited state of the ρ meson and is computed as follows:

$$\begin{aligned} \mathcal{C} \;=\; & 2\pi \frac{|\mathcal{A}|^2}{\int |\mathcal{A}|^2 dm_V} \frac{\mathrm{d}\sigma(AA \to AAV \to AA\pi^+\pi^-\pi^+\pi^-)}{\mathrm{d}^2 b \mathrm{d}y_V} \mathrm{d}m_V \mathrm{d}y_V \mathrm{d}b \\ / & \left[\frac{\mathrm{d}\sigma(AA \to AAV \to AA\pi^+\pi^-\pi^+\pi^-; y_{\pi_1} y_{\pi_2})}{\mathrm{d}y_{V_1} \mathrm{d}m_{V_1}} (1 - z_{\pi_1}^2) \mathrm{d}y_{V_1} \mathrm{d}m_{V_1} \right] \\ / & \left[\frac{\mathrm{d}\sigma(AA \to AAV \to AA\pi^+\pi^-\pi^+\pi^-; y_{\pi_3} y_{\pi_4})}{\mathrm{d}y_{V_2} \mathrm{d}m_{V_2}} (1 - z_{\pi_3}^2) \mathrm{d}y_{V_2} \mathrm{d}m_{V_2} \right] . \end{aligned} \tag{12}$$

The normalization takes into account the so-called a weight, which depends on the angle of vertical dispersion, $\sin^2(\theta)$. The normalization factor is equal to 1 for the case when pions are measured in full range. Then the total cross section for the production of four pions is equal to the total cross section for the production of a meson that decays into the four-pion state under study.

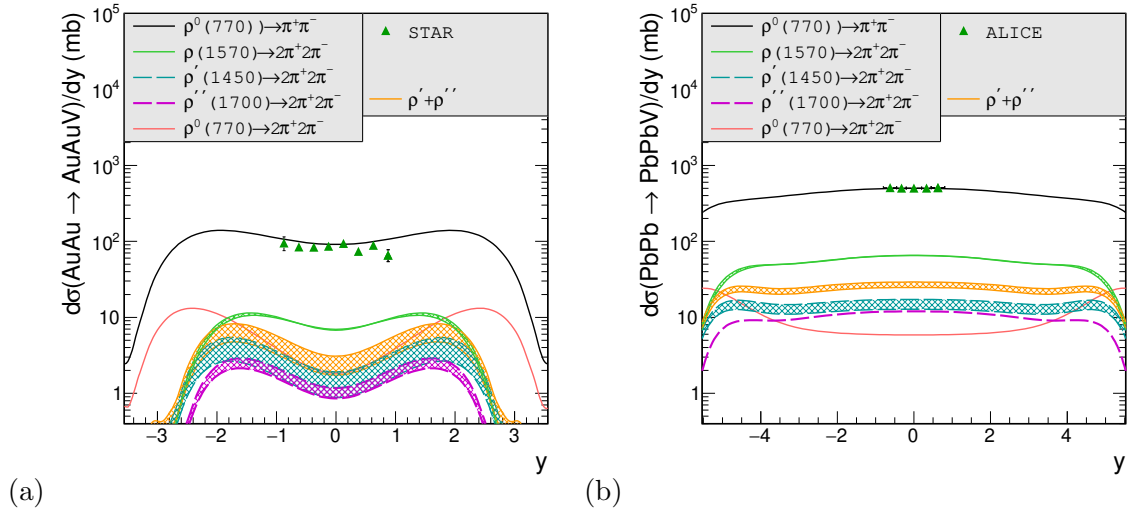

Figure 3 – Differential cross section as a function of rapidity of vector meson that decays into two or four charged pions. Results for $\pi^+\pi^-$ production are compared to the STAR data [35] (a) and the ALICE data [36] (b).

Fig. 3 presents the results for ultraperipheral $Au - Au$ collisions at $\sqrt{s_{NN}} = 200$ GeV (a) and Pb–Pb collisions at $\sqrt{s_{NN}} = 5.02$ TeV (b). the photoproduction of the $\rho(770)$ meson, which decays into two charged pions (represented by the upper black line), as well as the photoproduction of other vector meson ($\rho(1570)$ - solid green line, $\rho(1450)$ - dashed blue line, $\rho(1700)$ - dashed purple line, $\rho^0(770)$ - solid red line) are shown. As with the results in Fig. 2, uncertainties related to $V - \gamma$ coupling constant are indicated. The combined contribution from the ρ' and ρ'' is also highlighted (orange band). It is evident that the contribution for $\rho^0(770) \to \pi^+\pi^-\pi^+\pi^-$ state plays a significant role across a wide range of the meson rapidity at STAR, but it becomes less prominent at forward rapidities. The cross section for the production of four-charged-pion is largest in the case of $\rho(1570)$ meson decay.

The STAR Collaboration reported on the photoproduction of four pions in ultraperipheral $Au - Au$ collisions at $\sqrt{s_{NN}} = 200$ GeV [2], measuring pions at mid-rapidity, $|y_\pi| < 1$. Fig. 4 shows the four-pion invariant mass distribution, comparing the STAR data with our calculation. It also illustrated the

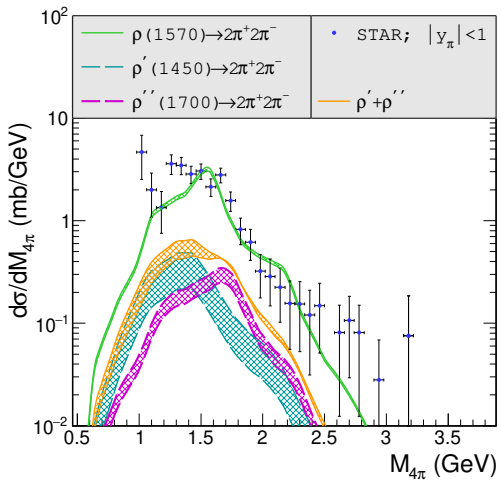

Figure 4 – Differential cross section as a function of four pion invariant mass.

contribution from the double-scattering ρ^0 mechanism discussed in Ref. [34], which accounts for approximately 20% of the measured cross section. Four-pion production can be also attributed to the subprocess $\gamma\gamma \to \rho^0\rho^0$, Ref. [37]. However, the cross section for the reaction $AuAu \to AuAu\rho^0\rho^0 \to AuAu2\pi^+2\pi^-$ is approximately two orders of magnitude smaller than the cross section measured by STAR. Fig. 4 also shows distributions for ρ', ρ'', their combined sum, and $\rho(1570)$. A correction for the acceptance function described in [34] has been applied. We find good agreement with the experimental data, particularly in terms of the decay of the $\rho(1570)$ resonance, which closely matches the STAR data. The shape of the four-pion invariant mass is strongly influenced by the Breit-Wigner description. In other words, the profile of the resonance smearing depends on the background correction factor, although the normalization of the smearing mass function remains consistent regardless of this factor. Although the H1 has also reported the four-pion invariant mass distribution, additional data is needed for direct comparison with our calculation. The sum of incoherent $\rho^{'}$ and $\rho^{''}$ mesons results in a cross section range of $0.41-0.74$ mb. The coherent sum of the mesons includes two $e^{i\varphi}$ factors in the Breit-Wigner formula. The first phase corresponds to the ρ' resonance, while the second phase φ_2 pertains to ρ''. The shape of the invariant mass is heavily dependent on the phase. The experimental cross section within $|y| < 1$ is measured at $\sigma = 2.4 \pm 0.2 \pm 0.8$ mb. The theoretical result for the $AuAu \to AuAu\rho(1570)(\to \pi^+\pi^-\pi^+\pi^-)$ process gives a range between $(2.16 - 2.31)$ mb.

Table 2: Ratio of the total cross section for the production of exclusive $\pi^+\pi^-\pi^+\pi^-$ to exclusive $\pi^+\pi^-$ in ultra-peripheral heavy ion collisions at $\sqrt{s_{NN}} = 200$ GeV and $\sqrt{s_{NN}} = 5.5$ TeV.

	$Au-Au$ at $\sqrt{s_{NN}} = 200$ GeV		$Pb-Pb$ at $\sqrt{s_{NN}} = 5.5$ TeV	
Resonance	$\lvert y_\pi\rvert < 10$	$\lvert y_\pi\rvert < 1$	$\lvert y_\pi\rvert < 10$	$\lvert y_\pi\rvert < 1$
$\rho(1450)$	$(2.1-2.8)\%$	$(1.9-2.5)\%$	3.7%	3%
$\rho(1570)$	$(5.8-6.2)\%$	8.2%	11.6%	13%
$\rho(1700)$	1.2%	1.3%	2.3%	2.4%
experimental data	$(13.4 \pm 4.5)\%$	$(16.4 \pm 5.3)\%$		

Given the strong agreement between the STAR data and our calculations, we now discuss predictions for LHC energies. Table 2 shows the ratio of total cross sections for the photoproduction of exclusive four-charged-pion to two-charged-pion states. The collision energies correspond to RHIC and LHC energies, with results provided for two intervals of pion rapidity: mid-rapidity in the range $(-1, 1)$ and $(-10, 10)$. Our predictions are compared with those from RHIC [2]. The cross sections are calculated using the decay width ranges specified in Table 1.

4 Summary and conclusions

We have presented the results from a simple model for the photoproduction of vector mesons that decay into the pion states. By incorporating a parametrization of recent preliminary data from the H1 Collaboration, this work enhances our understanding of the role of the ρ' and ρ'' resonances, as well as the $\rho(1570)$ meson, in exclusive four-pion production. Our study reveals that the $\rho(1570) \to \pi^+\pi^-\pi^+\pi^-$ process is dominant in the ultraperipheral heavy-ion collisions. A single ρ' or ρ'' resonances appears sufficient to describe the data. This work also highlights the significance of the broad $\rho(1570)$ resonance into the $AuAu \to AuAu\pi^+\pi^-\pi^+\pi^-$ process. The primary objective of this analysis was to offer specific predictions for LHC energies.

Recently, the ALICE Collaboration measured the cross section of exclusive four-pion photoproduction in ultraperipheral $Pb-Pb$ collisions at $\sqrt{s_{NN}} = 5.02$ TeV, Ref. [38]. The integrated four-pion cross section over the invariant mass range (0.8–2.5) GeV was found to be $d\sigma/dy = 47.8 \pm 2.3$ (stat.) ± 7.7 (syst.) mb at midrapidity $|y| < 0.5$. The peak around the invariant mass 1.5 GeV aligns with results reported by the STAR Collaboration. ALICE's data showes a better agreement with the two-resonance scenario than with the $\rho(1570)$. However, the data diverged by 2.1σ from our calculations based on a single resonance, as suggested by the H1 Collaboration. The ratio of the cross sections of ρ to ρ^0 is lower than measured by STAR in the events with mutual nuclear excitation.

Acknowledgments

I would like to thank Daniel Tapia-Takaki and Gerardo Herrera, co-chairs of the conference, for making the idea of organizing the first international workshop on the physics of Ultra Peripheral Collisions. This work has been supported by the Polish National Science Center grant DEC-2021/42/E/ST2/00350.

References

1. H1 Collaboration, S. Schmitt, 26th International Workshop on Deep Inelastic Scattering and Related Subjects (DIS 2018): Port Island, Kobe, Japan, April 16-20, 2018.
2. STAR Collaboration, B.I. Abelev et al., Phys. Rev. **C81** (2010) 044901 doi:10.1103/PhysRevC.81.044901
3. M. Klusek-Gawenda and J.D. Tapia Takaki, Acta Phys. Polon. **B51** (2020) 6, 1393 doi:10.5506/APhysPolB.51.1393
4. J.J. Sakurai, Annals Phys. 11 (1960) 1 doi:10.1016/0003-4916(60)90126-3
5. M. Gell-Mann and F. Zachariasen, Phys. Rev. **124** (1961) 953 doi:10.1103/PhysRev.124.953
6. A. Donnachie, P.V. Landshoff, Phys. Lett. **B296** (1992) 227 doi:10.1016/0370-2693(92)90832-O
7. CMS Collaboration, A. M. Sirunyan et al., Eur. Phys. J. **C79** (2019) 8 doi:10.1140/epjc/s10052-019-7202-9",
8. D. G. Cassel et al., Phys. Rev. **D24** (1981) 2787 doi:10.1103/PhysRevD.24.2787
9. E665 Collaboration, M. R. Adams et al., Z. Phys. **C74** (1997) 237 doi:E665:1997qph
10. CLAS Collaboration, C. Hadjidakis et al., Phys. Lett. **B605** (2005) 256 doi:10.1016/j.physletb.2004.11.019
11. CLAS Collaboration, S. A. Morrow et al., Eur. Phys. J. **A39** (2009) 5 doi:10.1140/epja/i2008-10683-5
12. H1 Collaboration, S. Aid et al., Nucl. Phys. **B463** (1996) 3 doi:10.1016/0550-3213(96)00045-4",
13. ZEUS Collaboration, J. Breitweg et al., Eur. Phys. J. **C2** (1998) 247 doi:10.1007/s100520050136
14. H. H. Bingham et al., Phys. Lett. **41B** (1972) 635 doi:10.1016/0370-2693(72)90653-3
15. M. Davier, et al., Nucl. Phys. **B58** (1973) 31 doi:10.1016/0550-3213(73)90545-2
16. P. Schacht, et al., Nucl. Phys. **B81** (1974) 205 doi;10.1016/0550-3213(74)90164-3
17. M. S. Atiya, et al., Phys. Rev. Lett. **43** (1979) 1691 doi:10.1103/PhysRevLett.43.1691
18. D. Aston, et al., Nucl. Phys. **B189** (1981) 15 doi:10.1016/0550-3213(81)90079-1
19. Particle Data Group, M. Tanabashi et al., Phys. Rev. **D98** (2018) 030001 doi:10.1103/PhysRevD.98.030001
20. T. H. Bauer, et al., Rev. Mod. Phys. **50** (1978) 261. [Erratum: Rev. Mod. Phys.51,407(1979)] doi:10.1103/RevModPhys.50.261
21. R. Glauber, *Lectures in theoretical physics*, vol.1. W.e. brittin, l.g. dunham (eds.), Interscience Publisher Inc., New-York.
22. S. Klein and J. Nystrand, Phys. Rev. **C60** (1999) 014903 doi:10.1103/PhysRevC.60.014903

23. H. De Vries, C. W. De Jager, and C. De Vries, Atom. Data Nucl. Data Tabl. **36** (1987) 495 doi:10.1016/0092-640X(87)90013-1
24. M. Kłusek-Gawenda and A. Szczurek, Phys. Rev. **C82** (2010) 014904 doi:10.1103/PhysRevC.82.014904
25. J. Contreras and J.D. Tapia Takaki, Int. J. Mod. Phys. A **30** (2015), 1542012 doi:10.1142/S0217751X15420129
26. M. Kłusek-Gawenda and A. Szczurek, Phys.Rev. **C93** (2016) 044912 doi:10.1103/PhysRevC.93.044912
27. M. Kłusek-Gawenda, PhD thesis, *Production of pairs of mesons, leptons and quarks in ultraperipheral ultrarelativistic heavy ion collisions*, Kraków, 2015.
28. STAR Collaboration, C. Adler et al., Phys.Rev.Lett. 89 (2002) 272302 doi:10.1103/PhysRevLett.89.272302
29. STAR Collaboration, B. I. Abelev et al., Phys. Rev. **C77** (2008) 034910.
30. STAR Collaboration, G. Agakishiev et al., Phys. Rev. **C85** (2012) 014910 doi:10.1103/PhysRevC.77.034910
31. ALICE Collaboration, J. Adam et al., JHEP 09 (2015) 095 doi:10.1007/JHEP09(2015)095
32. L. Frankfurt,V. Guzey, M. Strikman and M. Zhalov, Phys. Lett. **B752** (2016) 51 doi:10.1016/j.physletb.2015.11.012
33. J. Cepila, J.G. Contreras, M. Krelina and J.D. Tapia Takaki, Nucl. Phys. **B934** (2018) 330 doi:10.1016/j.nuclphysb.2018.07.010
34. M. Kłusek-Gawenda and A. Szczurek, Phys. Rev. **C89** (2014) 024912 doi:10.1103/PhysRevC.89.024912
35. STAR Collaboration, B.I. Abelev, Phys.Rev. **C77** (2008) 034910 doi:10.1103/PhysRevC.77.034910
36. ALICE Collaboration, S. Acharya et al., JHEP 06 (2020) 035 doi: 10.1007/JHEP06(2020)035
37. M. Kłusek and A. Szczurek, Phys.Lett.B 674 (2009) 92 doi:10.1016/j.physletb.2009.03.006
38. ALICE Collaboration, S. Acharya et al., arXiv: 2404.07542 [nucl-ex]